Acta Biochimica Polonica

Vol. 46 No. 3/1999

665-671

QUARTERLY

Factors improving the accuracy of determination of ^{15}N relaxation parameters in proteins*°

Igor Zhukov and Andrzej Ejchart✉

Institute of Biochemistry and Biophysics, Polish Academy of Sciences, A. Pawińskiego 5A, 02-106 Warszawa, Poland

Received: 23 June, 1999

Key words: ^{15}N relaxation, nuclear relaxation parameter accuracy, squash trypsin inhibitor

A number of factors at all stages of data processing which affect the accuracy of determination of ^{15}N relaxation parameters in ^{15}N-labeled proteins is discussed. Methods which allow to improve accuracy of the determined parameters are presented using data obtained for *Cucurbita maxima* trypsin inhibitor.

Recently the relationship between the internal dynamics of macromolecules and their biological functions has been the subject of much research [1, 2]. ^{13}C and/or ^{15}N relaxation measurements provide unique experimental data for characterization of intramolecular motions over a wide range of time scale [3, 4]. Information about the dynamics of a protein from the ^{15}N NMR relaxation studies is typically based on the measurements of ^{15}N longitudinal (T_1) and transverse (T_2) relaxation times and the steady-state heteronuclear $^{15}N\{^1H\}$ Overhauser enhancement (NOE) giving access to the mobility of N-H vectors [5, 6]. Sufficiently good accuracy of those relaxation parameters is crucial in further steps of the analysis of molecular motions.

General rules for optimal design and processing of relaxation measurements have been worked out for one-dimensional pulse sequences [7-9] and they remain valid for multidimensional NMR techniques as well. There is, however, a number of factors at all stages of processing of relaxation data for biological molecules which should be especially carefully taken into account due to their strong influence on accuracy of the relaxation parame-

*Presented at the symposium "Conformation of peptides, proteins and nucleic acids" held in Rynia, Poland, on 26-29 May, 1999.

°This work was financially supported by grant 6 P04A 009 16 from the State Committee for Scientific Research (KBN).

✉Correspondence to: Andrzej Ejchart, phone/fax: (48 22) 658 4683; e-mail: aejchart@ibb.waw.pl

Abbreviations: NMR, nuclear magnetic resonance; NOE, nuclear Overhauser enhancement; CMTI-I, *Cucurbita maxima* trypsin inhibitor type I.

ters. Sufficiently fine spectral digitization, efficient baseline correction, and careful choice of threshold and integration limits during processing of NMR spectra are of special importance. Data reduction leading to the experimental values of relaxation parameters also requires some precaution. Separate T_1 and/or T_2 measurements should be processed together with the use of a multiparameter nonlinear least-squares procedure [10]. Dynamic NOE measurements [11] are preferred over steady-state NOE ones as they allow to save total experimental time and to improve accuracy. The factors mentioned above have been analyzed and their importance evaluated using T_1, T_2 and NOE measurements performed for a small protein, the Met8→Leu mutant of squash trypsin inhibitor, CMTI-I (M8L), composed of 29 amino-acid residues. Nevertheless, it should be stressed that an ill-designed and/or ill-performed experiment cannot be saved by applying sophisticated processing methods.

MATERIALS AND METHODS

NMR sample. ^{15}N-labeled CMTI-I (M8L) recombinant protein was obtained by expression of a synthetic gene in *Escherichia coli* as described previously [12] and growing bacteria on glucose and ^{15}N ammonium sulfate as the only source of nitrogen. The protein was purified by reversed-phase HPLC. All experiments were performed at 303 K on a 3 mM ^{15}N-labeled protein sample in a solution containing 100 mM NaCl (pH = 7.0) and 10% D_2O. NMR spectra were acquired on a Varian Unity+ 500 MHz spectrometer equipped with a 5 mm triple-resonance gradient probe.

NMR experiments. The gradient sensitivity enhanced HSQC pulse sequence [13] with options for T_1, T_2 and $T_{1\rho}$ measurements of ^{15}N nuclei [14] was used to determine $T_1(^{15}N)$ and $T_2(^{15}N)$ values. $^{15}N\{^1H\}$ steady-state and dynamic NOEs were measured with a pulse sequence included in Varian Vnmr 6.1 software. Evolution time in two sets of T_1 measurements was set to the following values: 10, 30, 50, 90, 130, 210, 290, 410, 530, 650, 770, 890 ms and 10, 40, 60, 80, 100, 140, 180, 320, 440, 660 ms, respectively. For T_2 measurements, a Carr–Purcell–Meiboom–Gill pulse (CPMG pulse) train with refocusing delay of 625 μs was used during the evolution delay. T_2 values were obtained from two experiments with evolution times of 10, 30, 50, 90, 130, 190, 250 ms and 10, 30, 50, 90, 130, 170, 230, 290 ms, respectively. The delay between the 180°(^{1}H) pulses used to suppress cross-correlation effects [15] was 5 and 10 ms for the T_1 and T_2 measurements, respectively. In dynamic NOE measurements ^{1}H presaturation time was set to: 0, 80, 200, 600 and 2100 ms. All spectra were recorded with a spectral width of 1500 Hz in the F_1 dimension and of 6000 Hz in the F_2 dimension. 2048 and 256 complex data points in time domain were collected in the phase sensitive hypercomplex mode [16] with 16 scans (T_1 and T_2) or 24 scans (NOEs) per t_1 increment. A recycling delay of 1.6 s (T_1 and T_2) and 3 s (steady-state and dynamic NOE) was employed and ^{15}N decoupling during acquisition of data was performed using 3.2 kHz GARP sequence [17]. All NMR data were processed using NMRPipe software [18]. Spectra were transformed by applying cosine squared bell weighting function in both time dimensions with 4Kx2K points in the F_2 and F_1 dimensions, respectively. Analysis of two-dimensional spectra and cross-peak integration was performed using the XEASY program [19]. Relaxation parameters were determined by fitting the cross-peak integrals as a function of evolution time to a single-exponential decay.

RESULTS AND DISCUSSION

Baseline correction

The quantitative use of NMR spectroscopy requires accurate peak integration. In turn,

the integrals are very sensitive to small changes in the baseline of the spectrum. Baseline corruption can arise from several sources and it is inherent in many NMR experiments [20]. On the other hand, the accuracy of relaxation data can be strongly deteriorated due to improperly performed baseline correction. Despite a certain arbitrariness, a baseline correction is usually carried out in the frequency domain by fitting the baseline to a polynomial which may then be subtracted. If a baseline correction in two-dimensional spectra becomes doubtful one can resort to partial projections of one-dimensional spectra obtained as sums of all traces showing a given correlation signal. Baseline correction and integration procedures in NMR application softwares usually work more efficiently in the case of one-dimensional spectra than of two-dimensional ones. This is demonstrated by standard errors of T_1 and T_2 data obtained for six amino-acid residues of the CMTI-I (M8L) protein (Fig. 1). These residues were chosen because they exhibited the lowest signal to noise ratios and, thus, the highest relaxation time inaccuracies within the whole set of data. Inappropriate baseline correction procedure resulted in decreased accuracy of data as compared with that without baseline correction. Use of partial projections, however, allowed to improve data accuracy.

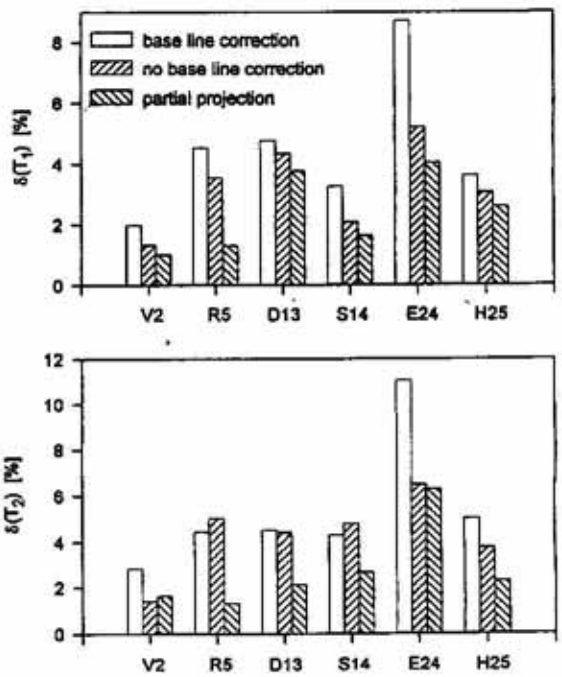

Figure 1. Standard errors of T_1 and T_2 data obtained for six amino acid residues of CMTI-I (M8L) protein, displaying the lowest signal to noise ratios.

Inappropriate baseline correction of two-dimensional spectra resulted in a larger scatter of data and increased standard error. On the other hand, calculation of partial projections followed by baseline correction of one-dimensional spectra improved the accuracy of calculated parameters.

Choice of threshold

In multidimensional spectra, peaks below a given level are routinely discarded in order to avoid excessive noise. The cutoff limit called a threshold is usually adjusted well above an average noise amplitude. Adjustment of the threshold, similarly as a distorted baseline, strongly influence the determined values of relaxation times. In order to demonstrate this influence, the Lorentzian signals (halfwidth equal to 1 Hz) were calculated for six evolution times, t, in simulated $T_{1,2}$ experiments and plotted within the range ±5 Hz (Fig. 2a). Integrals of those signals calculated for three threshold positions were used as input data for the calculations of relaxation times.

Shift of threshold brings about significant changes of calculated relaxation times T_{calc}. They differ from the value assumed in simulations (T = 1 s) much more than one could expect from their standard deviations (Fig. 2b). Intensity changes *vs.* evolution time are not single-exponential any more and particular deviations of data points from curves calculated by nonlinear least-squares procedure are opposite for too high (A) and too low (C) threshold adjustment (Fig. 2c).

Collective data processing

For longitudinal (T_1) and transverse (T_2) relaxation times it can happen that measure-

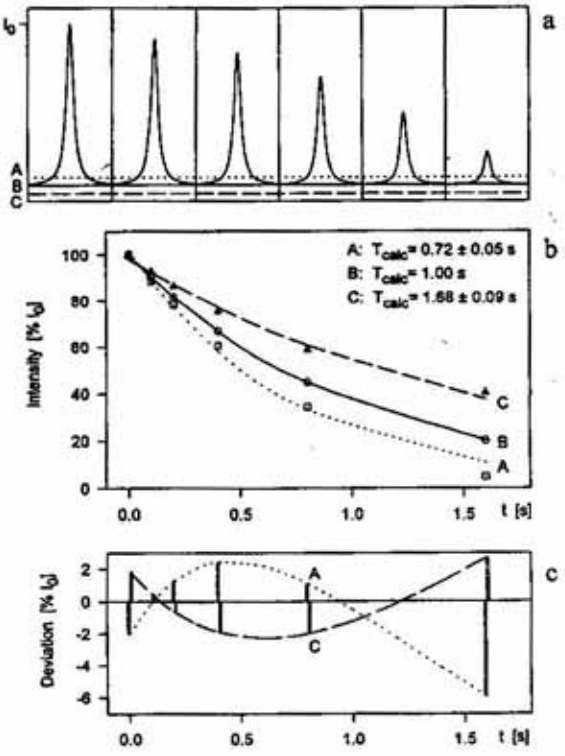

Figure 2. (a) Artificially generated Lorentzian signals with halfwidth of 1 Hz plotted within the range of ±5 Hz which mimic signal decay in a relaxation time experiment (assumed T = 1 s).

Horizontal line B represents zero level, whereas lines A and C correspond to the threshold adjusted at height $0.05 \cdot I_0$ above and below line B, respectively; I_0 is a signal intensity at evolution time t = 0.

(b) Relaxation times calculated from signals presented in Fig. 2(a) which were integrated relative to three different zero levels.

Positive threshold (A) resulted in a decreased value of relaxation time, T = 0.72 s and negative threshold (C) resulted in an increased value, T = 1.68 s.

(c) Deviations of individual integrals from the best fits obtained for misadjusted threshold levels.

ments will not be feasible in a single approach owing to the necessity of extended measurement time if high resolution in indirectly detected dimension, sufficient number of evolution times and satisfactory signal to noise ratio are expected. In such a case, improvement in accuracy can be obtained by measuring a given relaxation time several times. Then it is far better to process collectively individual data sets using appropriate weighting factors, if necessary [10].

The relaxation times T_1 determined for CMTI-I (M8L) in two separate measurements exhibited smaller errors when processed together as shown in Fig. 3. The first and second measurement comprised 12 and 10 evolution times, respectively.

Improvement of NOE data accuracy

Accurate values of heteronuclear Overhauser effect are indispensable to the analysis of molecular motions in proteins. However, unexpected NOE values were measured occasionally in proteins [21–23] and no explanation could be given for such observations. Heteronuclear $^{15}N\{^1H\}$ Overhauser enhancements can be measured either in a steady-state or applying a progressive saturation (dynamic NOE). In the steady-state method NOE is calculated from the intensity ratios in two spectra measured either with or without ^1H saturation. Presaturation time or relaxation delay, t_d, should be much longer than the longest T_1 value in a molecule: $t_d > 5 \cdot T_1$ or, preferably, $t_d > 10 \cdot T_1$ [24]. Such measurement is usually repeated several times. On the other hand, in the dynamic NOE a series of spectra with increasing presaturation time of ^1H nuclei is measured. NOE builds up with a time constant equal to the relaxation time T_1. It should be pointed out that the T_1 values can be determined in a separate, high accuracy experiment. Therefore, dynamic NOE measurements can be processed either using T_1 data derived from separate measurements or NOE and T_1 raw data can be processed together. For this very reason a dynamic NOE measurement allows to determine NOE values more precisely than a steady-state measurement in a given experimental time.

NOEs for CMTI-I (M8L) were measured using both methods discussed (Fig. 4). Steady-

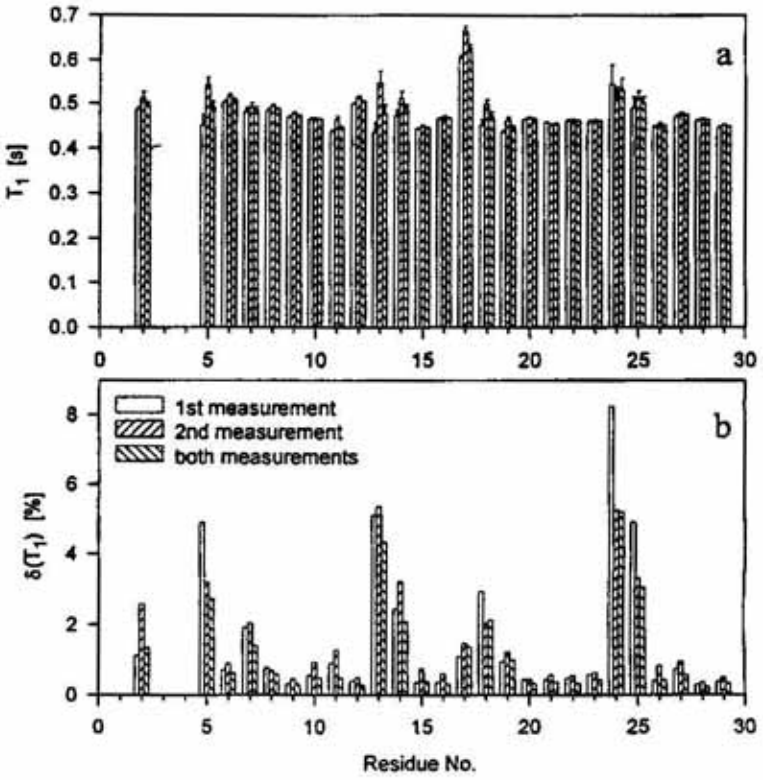

Figure 3. Experimental data of longitudinal relaxation times T_1 (a) and their standard errors (b) for CMTI-I (M8L) protein.

Two independent measurements were processed either separately or collectively. The latter processing allowed to improve the accuracy of data.

state results are averages of four separate measurements; total experimental time of eight 2D spectra was 111 h. The dynamic NOE measurement comprised five spectra obtained at different ^1H presaturation times; total experimental time of five 2 D spectra was

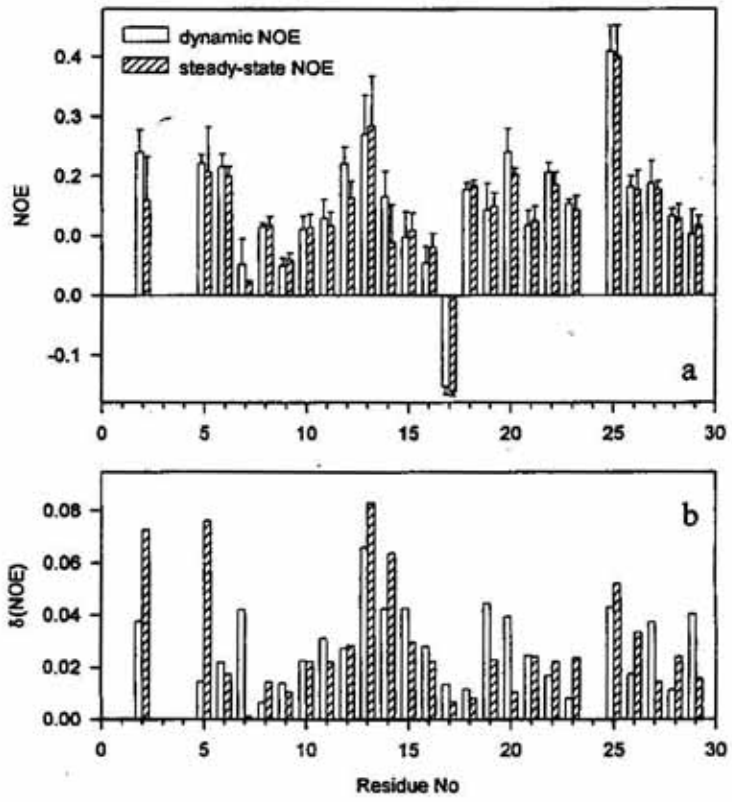

Figure 4. Experimental data of $^{15}N\{^1H\}$ nuclear Overhauser enhancements (a) and their standard errors (b) for CMTI-I (M8L) protein.

Two different experimental methods were used. In the dynamic method the NOEs values were calculated from five spectra obtained at different ^1H presaturation times with T_1 values derived from a separate measurement. The steady-state results were averages of four separate measurements.

70 h. Despite significantly shorter experimental time almost half of the NOE data calculated from the dynamic NOE experiment exhibited better accuracy than those determined by the steady-state method.

REFERENCES

1. Williams, R.J.P. (1989) NMR studies of mobility within protein structure. *Eur. J. Biochem.* **183**, 479–497.
2. Pabo, C.O. & Sauer, R.T. (1992) Transcription factors: Structural families and principles of DNA recognition. *Annu. Rev. Biochem.* **61**, 1053–1095.
3. Barbato, G., Ikura, M., Kay, L.E., Pastor, R.W. & Bax, A. (1992) Backbone dynamics of calmodulin studied by ^{15}N relaxation using inverse detected two-dimensional NMR spectroscopy: The central helix is flexible. *Biochemistry* **31**, 5269–5278.
4. Peng, J.W. & Wagner, G. (1992) Mapping of spectral density functions using heteronuclear NMR relaxation measurements. *J. Magn. Reson.* **98**, 308–332.
5. Kay, L.E., Torchia, D.A., & Bax, A. (1989) Backbone dynamics of proteins as studied by ^{15}N inverse detected heteronuclear NMR spectroscopy: Application to staphylococcal nuclease. *Biochemistry* **28**, 8972–8979.
6. Clore, G.M., Driscoll, P.C., Wingfield, P.T. & Gronenborn, A.M. (1990) Analysis of the backbone dynamics of interleukin-1β using two-dimensional inverse detected heteronuclear ^{15}N-^{1}H NMR spectroscopy. *Biochemistry* **29**, 7387–7401.
7. Weiss, G.H. & Ferretti, J.A. (1983) Accuracy and precision in the estimation of peak areas and NOE factors. *J. Magn. Reson.* **55**, 397–407.
8. Weiss, G.H., Ferretti, J.A. & Byrd, R.A. (1987) Accuracy and precision in the estimation of peak areas and NOE factors. II. The effects of apodization. *J. Magn. Reson.* **71**, 97–105.
9. Weiss, G.H. & Ferretti, J.A. (1988) Optimal design of relaxation time experiments. *Prog. NMR Spectrosc.* **20**, 317–335.
10. Gryff-Keller, A., Ejchart, A. & Jackowski, K. (1994) Shielding anisotropies of acetic carbons and solution molecular dynamics of ethynyltrimethylsilane as studied by ^{13}C nuclear spin relaxation and theoretical *ab initio* calculation. *J. Magn. Reson. A* **111**, 186–190.
11. Kowalewski, J., Ericsson, A. & Vestin, R. (1978) Determination of NOE factors using the dynamic Overhauser enhancement technique combined with a nonlinear least-squares-fitting procedure. *J. Magn. Reson.* **31**, 165–169.
12. Bolewska, K., Krowarsch, D., Otlewski. J., Jaroszewski, L. & Bierzyński, A. (1995) Synthesis, cloning and expression in *Escherichia coli* of a gene coding for the Met8→Leu CMTI-I – a representative of the squash inhibitors of serine proteinases *FEBS Lett.* **377**, 172–174.
13. Kay, L.E., Keifer, P. & Saarinen, T. (1992) Pure absorption gradient enhanced heteronuclear single quantum correlation spectroscopy with improved sensitivity. *J. Am. Chem. Soc.* **114**, 10663–10665.
14. Farrow, N.A., Muhandiram, R., Singer, A.U., Pascal, S.M., Kay, C.M., Gish, G., Shoelton, S.E., Pawson, T., Forman-Kay, J.D. & Kay, L.E. (1994) Backbone dynamics of a free and a phosphopeptide-complexed Src homology 2 domain studied by ^{15}N NMR relaxation. *Biochemistry* **33**, 5984–6003.
15. Kay, L.E., Nicholson, L.K., Delaglio, F., Bax, A. & Torchia, A. (1992) Pulse schemes for removal of the effects of cross correlation between dipolar and chemical-shift anisotropy relaxation mechanisms on the measurement of heteronuclear T_1 and T_2 values in proteins. *J. Magn. Reson.* **97**, 359–375.

16. States, D.J., Habercorn, R.A. & Ruben, D.J. (1982) A two-dimensional nuclear Overhauser experiment with pure absorptive phase in four quadrants. *J. Magn. Reson.* **48**, 286–292.

17. Shaka, A.J., Baker, P.B. & Freeman, R. (1985) Computer-optimized decoupling scheme for wideband applications and low-level operation. *J. Magn. Reson.* **64**, 547–552.

18. Delaglio, F., Grzesiek, S., Vuister, G.W., Zhu, G., Pfeifer, J. & Bax, A. (1995) NMRPipe: A multidimensional spectral processing system based on UNIX pipes. *J. Biomol. NMR* **6**, 277–293.

19. Bartels, C., Xia, T., Billeter, M., Güntert, P. & Wüthrich, K. (1995) The program XEASY for computer-supported NMR spectral analysis of biological macromolecules *J. Biomol. NMR* **6**, 1–10.

20. Cavanagh, J., Fairbrother, W.J., Palmer III, A.G. & Skelton, N.J. (1996) *Protein NMR Spectroscopy. Principles and Practice.* Academic Press, San Diego.

21. Bremi, T., Ernst, M. & Ernst, R.R. (1994) Side-chain motion with two degrees of freedom in peptides. An NMR study of phenylalanine side chains in antamanide. *J. Phys. Chem.* **98**, 9322–9334.

22. Rischel, C., Madsen, J.Chr., Andersen, K.V. & Poulsen, F.M. (1994) Comparison of backbone dynamics of apo- and holo-acyl-coenzyme A binding protein using ^{15}N relaxation measurements. *Biochemistry* **33**, 13997–14002.

23. Remerowski, M.L., Pepermans, H.A.M., Hilbers, C.W. & van de Ven, F.J.M. (1996) Backbone dynamics of the 269-residue protease Savinase determined from ^{15}N NMR relaxation measurements. *Eur. J. Biochem.* **235**, 629–640.

24. Canet, D. (1976) Systematic errors due to improper waiting times in heteronuclear Overhauser effect measurements by the gated decoupling technique. *J. Magn. Reson.* **23**, 361–364.